

PATTERNED NEURONAL NETWORKS FOR ROBOTICS, NEUROCOMPUTING, TOXIN DETECTION AND REHABILITATION

Jung F. Kang*, Matt Poeta, Lisa Riedel, Mainak Das, Cassie Gregory, Peter Molnar, James J. Hickman

Nanoscience Technology Center, University of Central Florida, Orlando, FL 32826

ABSTRACT

Biological systems can, in many aspects, be superior to existing control, computing, and warfare-agent detection systems. On the other hand, silicon-based electronics have many benefits over biological systems. Thus, an ideal system could use concepts and solutions from both biological and engineering principles. In this study we have developed basic methods to create hybrid neuronal systems consisting of single neurons or a simple neuronal network integrated with silicon-based electronics. We used the Self Assembled Monolayers (SAMs), DETA (trimethoxysilylpropyldiethylenetriamine) and 13F (tridecafluoro-1,1,2,2-tetrahydroctyl-1-trichlorosilane) in combination with deep *UV* photolithography to create surface patterns to determine cell attachment and dendritic/axonal growth. We have utilized the necessary methods to characterize these patterns and evaluated the survival and physiology of the patterned neurons. Elemental composition analysis using XPS, contact angle measurements and electroless metallization proved the formation of the surface patterns. The 'two cell networks', 'polarity determination', and 'axon-outgrowth' patterns successfully directed the adhesion, growth, and differentiation of embryonic rat hippocampal cells and motoneurons in serum-free culture media. The cultured cells displayed a compliance of more than 50% to the cell-adhesive patterns of the SAMs at 4-6 days *in vitro*. The neurons survived up to 35 days on the patterns. Immunostaining with MAP2 and Neurofilament, neuronal markers indicated that surface patterns alone can determine polarity of the neurons. Single and dual patch clamp electrophysiological recordings proved that the patterned neurons exhibited normal physiological properties and formed functional synaptic connections. In this study we successfully integrated living cells with silicon structures using standard tools which are compatible with industrial microchip manufacturing methods.

INTRODUCTION

Biological systems are in many aspects superior compared to existing control, computing, and warfare-agent detection systems (Zhang, Yang et al. 2004). For example, the precision utilized for movement control of higher-level biological organisms is very difficult to

reproduce with current control systems (Henson, Ogunnaike et al. 1994). Also, biological systems are in active interaction with their environment, and in this way they can be ideal biosensors (Bousse 1996). For example, endothelial cells, when attached to a peptide-modified cellulose membrane, can change the ion permeability in response to histamine, a toxin (May, Wang et al. 2004). Also, a whole cell microalgae, when immobilized inside a bovine serum albumin membrane, has been used as the enzyme-based bioreceptor for detection of cadmium ions and toxins in aquatic habitats (Celine Chouteau 2004). The idea of high throughput whole-cell biosensors have been discussed for many years (Kapur, Giuliano et al. 1999; Keusgen 2002). The neurons of the chick embryo, when seeded on microelectrode arrays, showed a change in its burst activity with two drugs, NBQX and CTZ (Chiappalone, Vato et al. 2003). On the other hand, engineered electronic systems can be much faster than biological systems, they can have higher computing capacity and their outputs and inputs can be standardized for connection to other subsystems. Thus, an ideal system would use concepts and solutions from both biological and engineering principles.

The major goal of our laboratory is to create hybrid neuronal systems consisting of single neurons or a simple neuronal network integrated with silicon-based electronics (Fromherz, Offenhausser et al. 1991; Hickman and Ravenscroft 1999; Hickman 2000; Fromherz 2002). We are using these engineered hybrid systems to 1) understand how simple physiological systems work, how neuronal networks can process information and how basic physiological control circuits function 2) exploring the possibilities for manipulating living cells *in vitro* and how to interface them with electronic systems 3) how to use living cells or networks as biosensors 4) and finally can we develop new strategies to enhance neuronal regeneration (Lucius, Mentlein et al. 1998) or return of physiological functions after injury. In this paper we report the development of the basic methods for the *in vitro* manipulation of living cells and their integration with silicon structures.

We have used surface chemistry (Das, Molnar et al. 2003) combined with advanced surface patterning techniques (Bhatia, Hickman et al. 1992), to engineer neuronal networks. Surface chemistry utilizing self-assembled monolayers (Laibinis, Hickman et al. 1989) (SAMs) is an excellent method to develop molecular-

Report Documentation Page

*Form Approved
OMB No. 0704-0188*

Public reporting burden for the collection of information is estimated to average 1 hour per response, including the time for reviewing instructions, searching existing data sources, gathering and maintaining the data needed, and completing and reviewing the collection of information. Send comments regarding this burden estimate or any other aspect of this collection of information, including suggestions for reducing this burden, to Washington Headquarters Services, Directorate for Information Operations and Reports, 1215 Jefferson Davis Highway, Suite 1204, Arlington VA 22202-4302. Respondents should be aware that notwithstanding any other provision of law, no person shall be subject to a penalty for failing to comply with a collection of information if it does not display a currently valid OMB control number.

1. REPORT DATE 00 DEC 2004	2. REPORT TYPE N/A	3. DATES COVERED -			
4. TITLE AND SUBTITLE Patterned Neuronal Networks For Robotics, Neurocomputing, Toxin Detection And Rehabilitation		5a. CONTRACT NUMBER g			
		5b. GRANT NUMBER			
		5c. PROGRAM ELEMENT NUMBER			
6. AUTHOR(S)		5d. PROJECT NUMBER			
		5e. TASK NUMBER			
		5f. WORK UNIT NUMBER			
7. PERFORMING ORGANIZATION NAME(S) AND ADDRESS(ES) Nanoscience Technology Center, University of Central Florida, Orlando, FL 32826		8. PERFORMING ORGANIZATION REPORT NUMBER			
9. SPONSORING/MONITORING AGENCY NAME(S) AND ADDRESS(ES)		10. SPONSOR/MONITOR'S ACRONYM(S)			
		11. SPONSOR/MONITOR'S REPORT NUMBER(S)			
12. DISTRIBUTION/AVAILABILITY STATEMENT Approved for public release, distribution unlimited					
13. SUPPLEMENTARY NOTES See also ADM001736, Proceedings for the Army Science Conference (24th) Held on 29 November - 2 December 2005 in Orlando, Florida., The original document contains color images.					
14. ABSTRACT					
15. SUBJECT TERMS					
16. SECURITY CLASSIFICATION OF:			17. LIMITATION OF ABSTRACT UU	18. NUMBER OF PAGES 8	19a. NAME OF RESPONSIBLE PERSON
a. REPORT unclassified	b. ABSTRACT unclassified	c. THIS PAGE unclassified			

level control over surface properties. Almost any surface can be derivatized with functionalized monolayers, which possess specific electrical (Hickman, Ofer et al. 1991; Collard 1999), optical (Evans, Johnson et al. 1998) or chemical (Bain, Troughton et al. 1989) properties. The most commonly used substrates are gold, glass, silicon or an elastomer, poly(dimethyl-siloxane). A wide variety of functional groups (Kang, Ulman et al. 2001) are available for surface modification. Self-assembled monolayers have already been used for the study of cell-surface interactions (Schaffner, Barker et al. 1995), cell patterning, control of protein adsorption (Schaffner, Barker et al. 1995) and prosthetic device biocompatibility (Puleo and Nanci 1999; Schoenfisch, Ovadia et al. 2000; Tosatti, Michel et al. 2002). SAMs are also compatible with standard photolithography methods. We have used a deep UV laser and a quartz mask to ablate defined areas of SAM-modified surfaces and use a second SAM to backfill the ablated area. In this way, we have created patterns where cells preferably adhere with a background where cells do not adhere (Kleinfeld, Kahler et al. 1988; Dulcey, Georger et al. 1991; Liua, Coulombe et al. 2000).

Surface chemistry using SAMs has evolved in the last fifteen years (Ulman 1991). Not only does the surface chemistry of the SAMs depend on their chemical functional groups but also the structure of the SAMs (Weiss, Yokota et al. 1998). The mixed SAMs of a ferrocenyl thiol and a quinone thiol on gold have been shown to work as pH microsensors (Hickman, Ofer et al. 1991). SAM patterns of disulfide and isocyanide were first created according to the patterns of platinum and gold (Hickman, Laibinis et al. 1992). Patterning of SAMs has been applied to guide the adsorption of the proteins (Bhatia S. K. 1993), and the adhesion and growth of the cells or neurons (Stenger 1992; Spargo 1994).

Dual patch-clamp (Neher and Sakmann 1992; Ravenscroft, Bateman et al. 1998) recording has been applied to investigate the cellular communication across the cell membranes through its ion channel or gated proteins (Powers and Binder 2000; Rekling, Funk et al. 2000); (Wilcox, Buchhalter et al. 1994; Mynlieff 1999) between two neighboring cells that adhered and developed on the patterned surface. Our results show that patterned surfaces can confine the functional synaptic connections to cells exclusively grown on a single pattern.

MATERIALS AND METHODS

Preparation of quartz-photomask. A 2-D design was drawn with computer-aided drafting (CAD) and then turned into a chromium pattern coated on a quartz plate. The quartz plate was then used as a photomask for ablating self-assembled monolayer (SAMs) according to the designed pattern. The processes of making the

photomask include camera filming, photoresist spin-coating, UV photolithography, and chemical-etching using a mixture of 12% nitric acid 10% ceric ammonium nitrate, and 78% water (Williams and Muller 1996).

The 2-D dimensions of the chromium pattern were later copied into a pattern of the SAMs with the use of the deep-UV laser. In the following experiments, the patterned SAMs were used to direct the adhesion, growth, and differentiation of embryonic rat hippocampal cells and motoneurons in cell culture. These designed patterns were aiming at 'two cell networks' (Figure 3), 'polarity determination' (Figure 4), and 'axon-outgrowth' (Figure 5).

Formation of SAMs patterns. A Surface was created with DETA (United Chemical Technologies) where cells could preferably adhere. A 193 nm Ar/F LPX200i laser beam (Lambda Physik, Ft. Lauderdale, FL) combined with a beam homogenizer (Microlas, Ft. Lauderdale, FL), was applied to ablate the SAMs for formation of the DETA pattern. The ablated area was backfilled with a second SAM of 13F (Gelest) on which cells do not adhere.

Surface characterization. Contact angle measurements were determined using a static, sessile drop (5 μ L) of deionized water with a CAM 200 digital goniometer (KSV Instruments, Ltd.). Three measurements were taken and averaged. High resolution XPS spectra were obtained using a Kratos AXIS165 XPS system equipped with monochromatic Al K α X-ray source. The pass energy of the analyzer and the take off angle of the photoelectron was set at 40eV and 90°. Survey scans and high-resolution scans for fluorine (1s), oxygen (1s), nitrogen (1s), carbon (1s) and silicon (2p) were performed for each sample. Based on the high-resolution scans, elemental composition percentages were calculated for each element using the following equations (Poeta, Riedel et al. 2004):

$$I_i = \Sigma I_{i_i} \quad (1)$$

$$I_i S = I_i / ASF \quad (2)$$

$$IS_T = \Sigma I_i S_i \quad (3)$$

$$At_i = (I_i S / \Sigma I_i S_i) * 100\% \quad (4)$$

Where I_i is the total area under one high-resolution scan curve and ΣI_{i_i} is the area under an individual curve fitted to the high-resolution scan. ASF is the atomic sensitivity factor, where 1.000, 0.780, 0.477, 0.278, and 0.328 were for fluorine (1s), oxygen (1s), nitrogen (1s), carbon (1s) and silicon (2p) respectively. IS_T is the summation of all of the high-resolution areas divided by their respective ASF and At_i is the elemental composition percentage. The At_i values for N (1s) in DETA controls was calculated, and the At_i values for F

(1s) in 13F controls was calculated. The A_t values for N (1s) and F (1s) in mixed SAMs were normalized with those for the control DETA and 13F. Thus the relative percent of the DETA and 13F in mixed SAMs were compared using the normalized A_t values for N (1s) and F (1s).

Electroless metallization. Patterned SAMs were visualized with electroless copper deposition (Kind, Bittner et al. 1998). In this method, shown in Figure 1, copper binds to the amine groups of the DETA through a series of chemical reactions. First the substrates were immersed in a PdCl_4^{2-} solution for 15 minutes. The solution was made of 10 mg of PdCl_4^{2-} and 1.75 gms of sodium chloride in 50 ml of water and the pH of the solution was adjusted to 1 with concentrated HCl. The palladium ions (PdCl_4^{2-}) bind to the amino groups on the surface during the step. They were then rinsed thoroughly with water and immersed for 15 minutes in a dimethylamine borane (DMAB) solution where 1.7 gms of DMAB is dissolved in 50 ml of water. The Pd^{+2} ions on the surface were reduced to Pd metal during this step. The samples were again rinsed thoroughly with water and then immersed in a copper bath solution. The copper bath solution was made of 3 grams of copper sulfate, 14 grams of sodium potassium tartrate and 2 grams of NaOH in 100 ml distilled water. In the copper bath solution, 100 μl of formaldehyde (37.2%) was added to 10 ml of copper solution for reducing the copper ions (Cu^{+2}) into Cu metal. The Pd metal that was primarily bound to the amino groups served as the precursor for deposition of the copper on the surface.

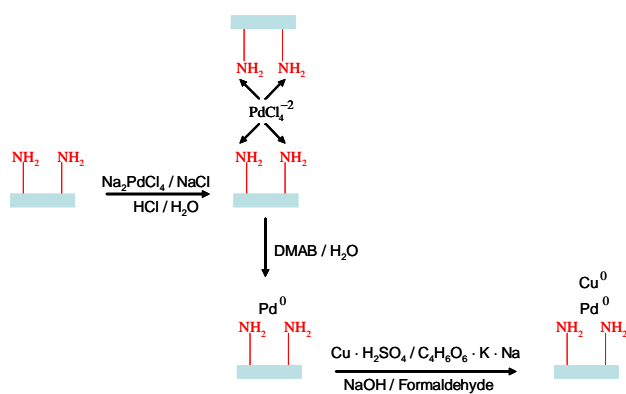


Figure 1: Electroless metallization

Plating cells on the SAM patterns. The hippocampal cells and motoneurons were purified prior to their plating on the patterned SAMs. Hippocampal cells and motoneurons were removed respectively from day 17 and day 14 rat fetuses after C-sectioning the pregnant mother rat. The hippocampi were collected in cold Hibernate E+ glutamine (0.5mM) + B27 supplement. The tissue was triturated using a sterile pasteur pipette. The dissociated tissue was centrifuged at 1000 rpm for 2 minutes. The pellet was resuspended in

growth medium. The growth medium consisted of Neurobasal (Invitrogen 21103-049) glutamine (0.5mM) + B27 supplement. Ventral spinal cells from the embryo were also dissociated after trypsin (Introgen, 0.05%) treatment and centrifugation for 15 minutes at 800g over a 6.5% metrizamide gradient. The large cells remaining above the cushion were further selected using the immune interaction between anti-NGF (Chemicon mAB 365) and the 192 antibody (1:2 dilution, ICN Biomedicals, Akron, OH) coated on the dishes. The antibody recognizes the low affinity NGF receptor expressed only by ventral motoneurons at this age. The purified hippocampal cells and motoneurons were plated on the patterned SAMs at a density of approximately 60-120 cells/ mm^2 in a serum-free culture media. The culture media contained versatile growth factors for hippocampal cells and motoneurons, respectively. The hippocampal media consisted of 500 ml Neurobasal media (Gibco), 10ml Gibco B-27 Supplement 50x, 1.25ml Glutamine (0.5 mM), 500 μl of 10ng/ml Recombinant Human Cardiotrophin-1 (Cell Science), 75 μl of 1 ng/ml Brain Derived Neurotrophic factors (Invitrogen), and 75 μl Glial Derived Neurotrophic Factor. The motoneuron media was Neurobasal media (Gibco-BRL) supplemented with B27 (2% v/v; Invitrogen), L-glutamine (0.5 mM), and 2-mercaptoethanol (25 μM), Glial cell line-Derived Neurotrophic factor (100 $\mu\text{g mL}^{-1}$ GDNF; Invitrogen), Brain Derived Neurotrophic factors (100 $\mu\text{g mL}^{-1}$ BDNF; Invitrogen), and ciliary neurotrophic factor (1 ng mL^{-1} CNTF; Cell Sciences).

Morphological analysis. Pictures of cells grown on the patterned surfaces were taken using an inverted microscope (Zeiss Axiovert 100), which was equipped with a video camera (DAGE-MTI DC-200 color camera 1/3 inch) and 4 \times , 10 \times , and 20 \times objectives. The 4 \times and 10 \times are used with brightfield while 20 \times are used with phase-contrast. The pictures were enhanced in Adobe Photoshop and analyzed using Photoshop image Software.

Immunocytochemistry. The motoneurons on the patterns were triply immunostained with the use of appropriate markers. Briefly, purified motoneurons on the patterned surfaces were fixed using cold methanol at -20°C for 15 minutes. The permeation of motoneurons was performed with 50 mM lysine plus 0.1% Triton X-100 for 15 minutes at room temperature. Nonspecific staining was blocked using 2% BSA and 3% Donkey serum in PBS for 30 minutes. The motoneurons were stained with primary, secondary, and nucleus antibodies. The motoneurons were consecutively incubated with primary antibodies at 4°C overnight, with secondary antibodies in the dark at room temperature for two hours, and with DAPI for 5 minutes. The motoneurons were dipped into four different dilutions of alcohol (50%,

75%, 90%, and 100%). One drop of mounting solution was put on a clean glass slide to mount the coverslip. The surface on which the cells were grown was face down. Enamel was used to seat the edges of the coverslips to the slide so that they would not move. The glass was stored in a freezer for later analysis. The primary antibodies, Rabbit Anti-NeuroFilament 150 Kd Polyclonal Antibody (Chemicon AB1981) and Mouse Anti-MAP2 a&b Monoclonal Antibody (Chemicon MAB378) were diluted respectively at 1:300 and 1:500 with the blocking solution (2% BSA and 3% Donkey serum in PBS). The secondary antibodies were Alexa Fluor donkey antirabbit 594 and Alexa Fluor donkey anti-mouse 488 that stain for axons and dendrites respectively. The secondary antibodies were diluted to 4 μ l/ml with the use of PBS. The 4',6-diamidino-2-phenylindole (DAPI), (Molecular Probes D1306), was diluted into a 300 nM solution with distilled water. The pictures of immunostained cells were taken with a commercial Nikon Coolpix 990 camera using the 40x objective of the Zeiss Axiovert 100 microscope equipped with epifluorescent illumination, and were also taken with a Zeiss LSM510 laser scanning confocal microscope. The laser scanning confocal microscope is uniquely used for Z-section imaging with high spatial resolution. The LSM 510 performed simultaneous multi-color imaging.

Electrophysiology. Whole-cell patch clamp recordings were performed in a recording chamber on the stage of a Zeiss Axioscope 2FS Plus upright microscope. The extracellular solution was neurobasal culture medium whose pH value was adjusted to 7.3 with HEPES. Voltage clamp and current clamp experiments were performed using a Multiclamp 700A amplifier (Axon, Union City, CA).

RESULTS AND DISCUSSIONS

The contact angles of water for the SAMs of DETA and 13F were $41 \pm 1^\circ$ and $110 \pm 1^\circ$ respectively, as shown in Figure 2a and 2b. Elemental composition analysis using XPS showed the presence of nitrogen or fluorine atoms, respectively, confirming the amino or perfluoro functional groups were exclusively present from these two different SAMs.

The replacement of the DETA by 13F after ablation in the background area of the designed pattern was also confirmed using contact angle measurement and XPS elemental analysis. The measurement of the water contact angle was $110 \pm 1^\circ$ for the background area, which was the same as that for the 13F control surface. XPS elemental analysis (Figure 3) was used to characterize the patterned and background areas. The values of the $N(1s)/(N(1s) + F(1s))$ and $F(1s)/(N(1s) + F(1s))$ ratios gauge the relative percent of the DETA and 13F, respectively, regarding to the backfilling process.

These results indicate that the pattern area is mainly DETA while the background area is mainly 13F with the cross contamination at 10% between these two areas.

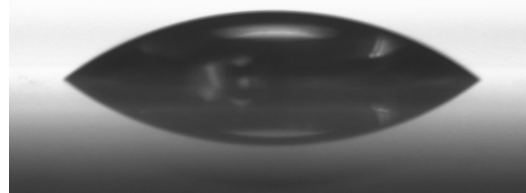


Figure 2a: Contact angle of DETA surface

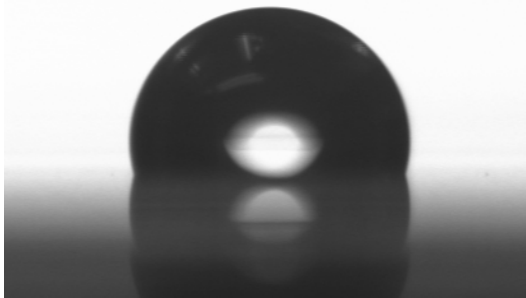


Figure 2b: Contact angle of 13F surface

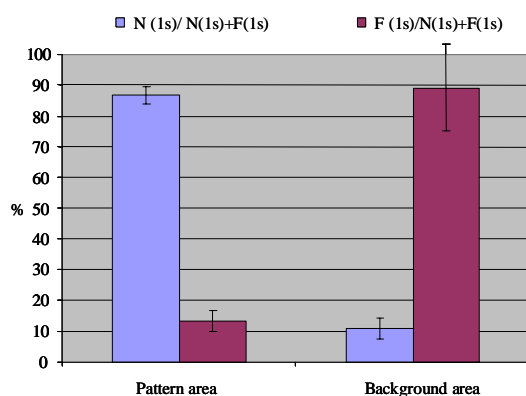


Figure 3: Elemental analysis by XPS, where the % corresponds to the relative percent of DETA and 13F

The patterned SAMs were also imaged with the use of a metallization technique. In these images, the DETA pattern on the 13F background was visualized as a pattern of the copper thin-film on the transparent surface. The image of the two cell network pattern is shown in Figure 4. The area (30 μ m in diameter) of a circle was designed to direct adhesion of the hippocampal cells; the solid line (7 μ m in width) was meant to direct the growth of the axons; and the dashed lines (7 μ m in width) were intended to slow down the growth of the hippocampal neurites in forming a dendrite. Thus, the hippocampal

neurons, when grown on a single pattern, are able to form directed functional synaptic connections.

The patterns for the polarity determination for the motoneurons were also intended to drive the growth of the axon and dendrites in different directions, as shown in Figure 5. The dashed lines (5 μm in width) were to encourage the growth of the dendrites while the solid lines (5 μm in width) were to guide the growth of the axons, which originated from the cell body in the circle. In this way, the motoneurons have an opportunity to individually grow to muscle cells in a co-culture of motoneuron and muscle. The images of the axon outgrowth pattern are shown in Figure 6. A large rectangular area (50 \times 400 μm) with branch lines (2 μm in width) that were in parallel were intended to drive multiple motoneurons to settle closely together so that the axons could grow into the lines, mimicking the growth of motoneurons from the inside of the spinal cord to its outside.

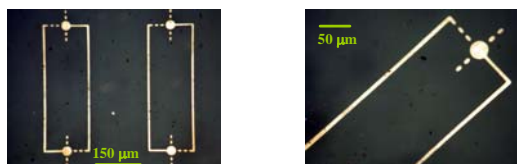
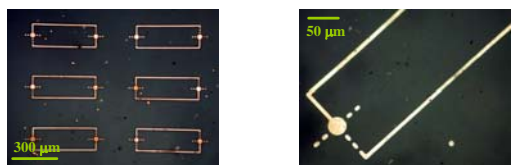


Figure 4: Metallization images (two cell network)

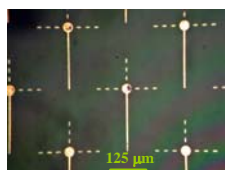
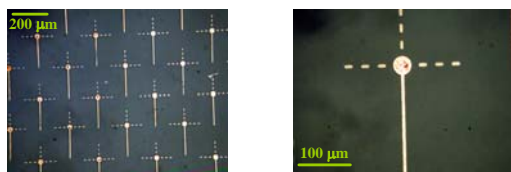


Figure 5: Metallization images (Polarity Determination)

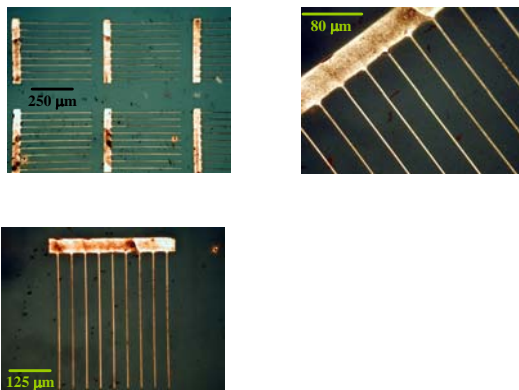


Figure 6: Metallization images (Axon outgrowth)

The cells cultured on the patterned surfaces were monitored on a daily basis. The morphology of the hippocampal cells grown on the ‘two cell networks’ pattern, and the morphology of the motoneurons grown on ‘polarity determination’ and the ‘axon-outgrowth’ patterns are shown in Figure 7, 8, and 9 respectively. The neuronal patterns of ‘two cell networks’, ‘polarity determination’, and ‘axon-outgrowth’ are shown at 4 \times , 10 \times , and 20 \times magnification. The micrographs were taken after 4-6 days in culture. The cells preferentially adhered on the pattern area and growth of neurites from the cell body began after one day of cell culture. The cells that fell on the 13F background were mostly detached from the surface after four days of culture. The morphology of the cells was fully developed after 4-6 days of cell culture. The cultured cells displayed a compliance (Corey, Wheeler et al. 1991) of more than 50% to the cell-adhesive surface at 4-6 days *in vitro*. The neurons survived up to 35 days on the patterns.

The hippocampal neurons formed a closed circuit (Figure 7) while the motoneurons demonstrated polarity without forming synaptic connections (Figure 8). In the axon outgrowth pattern, most of the motoneurons fell on the rectangle area and then grew processes along the branch lines in parallel (Figure 9).

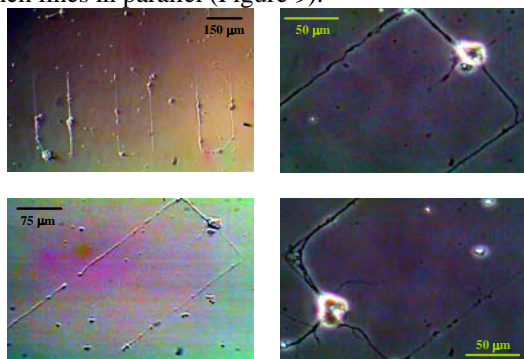


Figure 7: Two cell network

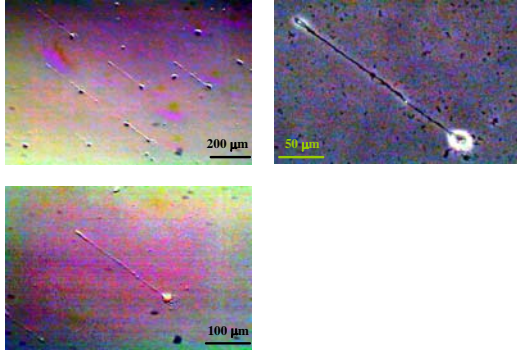


Figure 8: Polarity determination

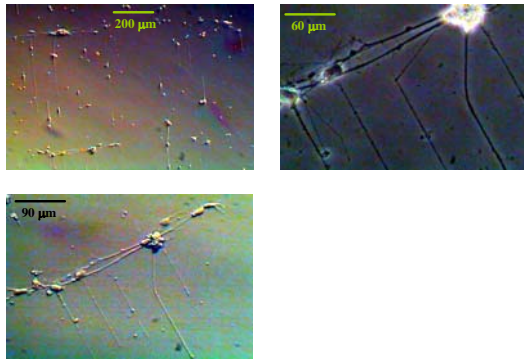


Figure 9: Axon outgrowth

It has been reported that Anti-NeuroFilament stains both axons and dendrites while Anti-MAP2 stains the dendrites (Dotti and Banker 1987) and DAPI stains nucleus exclusively. Therefore, the processes that stained positive and negative for anti-NeuroFilament and Anti-MAP2, respectively, were considered axons (Stenger, Hickman et al. 1998). The anti-NeuroFilament, Anti-MAP2, and DAPI were observed with red, green, and blue colors under the fluorescence microscope, as shown in Figure 10. These three colors point to the locations of the axons, the dendrites and cell body, respectively. In these images, a single motoneuron sat on a circle area of the pattern. The axon originated from the cell body extending on the solid line for as long as 200 μm , and more than one short dendrite developed in the vicinity of the cell body. The axonal/dendritic polarities of 6 and 9-day cultures on the patterns were compared using a confocal microscope. Micrographs of the 6 and 9-day cells taken are shown in Figures 11 and 12. In the Micrographs, the double immunostaining of the motoneurons clearly showed the major process, or axon, as well as the minor processes, or dendrites. The morphology and polarity of the motoneurons could be improved upon the reduction of the line width on the patterned surface, which will be discussed in a separate paper (Kang, Riedel et al. 2004).

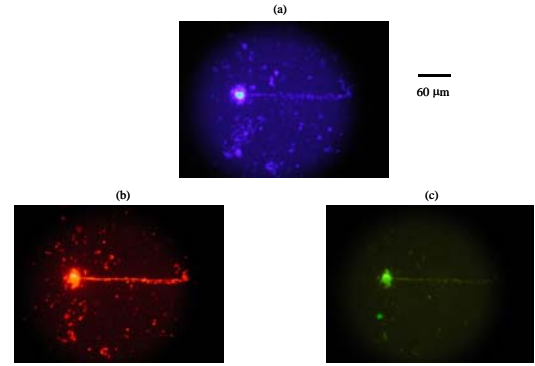


Figure 10: (a) Cell Body, (b) axon, and (c) dendrites

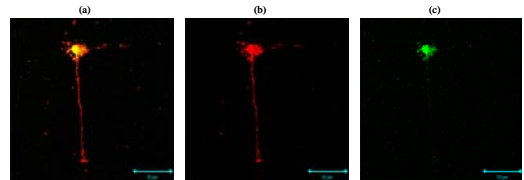


Figure 11: (a) Double immunostaining of axon and dendrites, (b) axon, and (c) dendrite after 6 days in cell culture. The scale bar is 50 μm

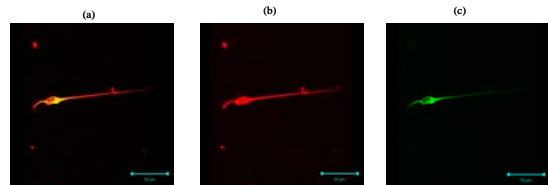


Figure 12: (a) Double immunostaining of axon and dendrites, (b) axon, and (c) dendrite after 9 days in cell culture. The scale bar is 50 μm

Dual patch-clamp electrophysiology was used to characterize the connectivity and synaptic transmission of neurons on the “two cell network” patterns. The dual patch clamp electrophysiological recordings proved that the patterned neurons exhibited normal physiological properties and formed functional synaptic connections.

CONCLUSIONS

In these studies we have developed the appropriate technology to manipulate neurons *in vitro*, created engineered neuronal networks and integrated single cells with silicon structures. These engineered functional neuronal systems can be used as model systems to study integration and behavior of neuronal networks, how small neuronal systems process information and how simple biological control circuits are organized and function. Combined with extracellular electrophysiological recordings they can also be used as the sensor element in high-throughput toxin and warfare-agent detection systems.

ACKNOWLEDGEMENT

We thank the support from NIH 1K01EB003465-01, NIH 1R21EB002307-01, South Carolina Spinal Cord Injury Research Grant 0403, DARPA Grant No. N65236-01-1-7400, DARPA Grant No. F30602-01-2-0541, and DOE Grants No. DE-FG02-00ER45856. We especially thank Prof. Jim Harriss in the Electrical Engineering Department of Clemson University for providing us his expertise and facility of his laboratory in making our quartz photomasks.

REFERENCES

- Bain, C. D., E. B. Troughton, et al. (1989). "Formation of Monolayer Films by the Spontaneous Assembly of Organic Thiols from Solution onto Gold." J. Am. Chem. Soc. **111**: 321-335.
- Bhatia S. K., T. J. L., Anderson M., Shriverlake L. C., Calvert J. M., Georger J. H., Hickman J. J., Dulcey C. S., Schoen P. E. and Ligler F. S. (1993). "Fabrication of Surfaces Resistant to Protein Adsorption and Application to Two-Dimensional Protein Patterning." Analytical Biochemistry **208**: 197-205.
- Bhatia, S. K., J. J. Hickman, et al. (1992). "New Approach To Producing Patterned Biomolecular Assemblies." J. Am. Chem. Soc. **114**: 4432-4433.
- BJ Spargo, M. T., TB Nielsen, DA Stenger, JJ Hickman and AS Rudolf (1994). "Spatially Controlled Adhesion, Spreading, and Differentiation of Endothelial Cells on Self-Assembled Molecular Monolayers." Proceedings of the National Academy of Sciences **91**: 11070-11074.
- Bousse, L. (1996). "Whole cell biosensors." Sensors and Actuators B **34**: 270-275.
- Celine Chouteau, S. D., Jean-Marc Chovelon, and Claude Durrieu (2004). "Development of novel conductometric biosensors based on immobilised whole cell *Chlorella vulgaris* microalgae." Biosensors and Bioelectronics **19**: 1089-1096.
- Chiappalone, M., A. Vato, et al. (2003). "Networks of neurons coupled to microelectrode arrays: a neuronal sensory system for pharmacological applications." Biosensors and Bioelectronics **18**: 627-634.
- Collard, S. I. a. D. M. (1999). "Chemical and Electrochemical Polymerization of 3-Alkylthiophenes on Self-assembled Monolayers of Oligothiophene-Substituted Alkylsilanes." Langmuir **15**: 3752-3758.
- Corey, J. M., B. C. Wheeler, et al. (1991). "Compliance of hippocampal neurons to patterned substrate networks." Journal of neuroscience research **30**: 300-307.
- Das, M., P. Molnar, et al. (2003). "Electrophysiological and Morphological Characterization of Rat Embryonic Motoneurons in a Defined System." Biotechnol. Prog. **19**: 1756-1761.
- David A. Stenger, J. H. G., Charles S. Dulcey, James J. Hickman, Alan S. Rudolph, Thor B. Nielsen, Stephen M. McCort, and Jeffrey M. Calvert (1992). "Coplanar molecular assemblies of amino- and perfluorinated alkylsilanes: characterization and geometric definition of mammalian cell adhesion and growth." J. Am. Chem. Soc. **114**: 8435-8442.
- Dotti, C. G. and G. A. Banker (1987). "Experimentally induced alteration in the polarity of developing neurons." Nature **330**: 254 - 256.
- Dulcey, C. S., J. J. Georger, et al. (1991). "Deep UV photochemistry of chemisorbed monolayers: patterned coplanar molecular assemblies." Science **252**: 551-4.
- Evans, S. D., S. R. Johnson, et al. (1998). "Photoswitching of Azobenzene Derivatives Formed on Planar and Colloidal Gold Surfaces." Langmuir **14**: 6436-6440.
- Fromherz, P. (2002). "Electrical Interfacing of Nerve Cells and Semiconductor Chips." ChemPhysChem **3**: 276 - 284.
- Fromherz, P., A. Offenhausser, et al. (1991). "A Retzius Cell of the Leech on an Insulated-Gate Field-Effect Transistor." Science **252**: 1290-1293.
- Henson, M. A., B. A. Ogunnaike, et al. (1994). "The Baroreceptor Reflex: A Biological Control System with Applications in Chemical Process Control." Ind. Eng. Chem. Res. **33**: 2453-2466.
- Hickman, J. J. (2000). "An apparatus for analysis of the electrophysiology of neuronal cells and its use in high throughput functional genomics." PCT Int. Appl. **72** pp. CODEN: PIXXD2 WO 2000071742 A2 20001130.
- Hickman, J. J., P. E. Laibinis, et al. (1992). "Toward Orthogonal Self-Assembly of Redox Active with Au and Isocyanide with Pt Molecules on Pt and Au: Selective Reaction of Disulfide." Langmuir **8**: 357-359.
- Hickman, J. J., D. Ofer, et al. (1991). "Molecular Self-Assembly of Two-Terminal, Voltammetric Microsensors with Internal References." Science **252**: 688-691.
- Hickman, J. J., D. Ofer, et al. (1991). "Selective functionalization of gold microstructures with ferrocenyl derivatives via reaction with thiols or disulfides: characterization by electrochemistry and Auger electron spectroscopy." J. Am. Chem. Soc. **113**: 1128-1132.
- Hickman, J. J. and M. S. Ravenscroft (1999). "Patterned neuronal networks for applications in biocomputing." Book of Abstracts, 217th ACS National Meeting.
- Jung, D. R., D. S. Cuttino, et al. (1998). "Cell-based sensor microelectrode array characterized by imaging x-ray photoelectron spectroscopy, scanning

- electron microscopy, impedance measurements, and extracellular recordings." Journal of Vacuum Science & Technology A: Vacuum, Surfaces, and Films **16**: 1183-1188.
- Kang, J. F., L. Riedel, et al. (2004). "Effect of line-width of the pattern surface on the polarity of the Motoneurons." In preparation.
- Kang, J. F., A. Ulman, et al. (2001). "Self-Assembled Rigid Monolayers of 4 ϕ -Substituted-4-mercaptobiphenyls on Gold and Silver Surfaces." Langmuir **17**: 95-106.
- Kapur, R., K. A. Giuliano, et al. (1999). "Streamlining the Drug Discovery Process by Integrating Miniaturization, High Throughput Screening, High Content Screening, and Automation on the CellChipTM System." Biomedical Microdevices **2**: 99-109.
- Keusgen, M. (2002). "Biosensors: new approaches in drug discovery." Naturwissenschaften **89**: 433-444.
- Kind, H., A. M. Bittner, et al. (1998). "Electroless Deposition of Metal Nanoislands on Amino-thiolate-Functionalized Au(111) Electrodes." J. Phys. Chem. B **102**: 7582-7589.
- Kleinfeld, D., K. H. Kahler, et al. (1988). "Controlled outgrowth of dissociated neurons on patterned substrates." Journal of Neuroscience **8**: 4098-120.
- Laibinis, P. E., J. J. Hickman, et al. (1989). "Orthogonal Self-Assembled Monolayers: Alkanethiols on Gold and Alkane Carboxylic Acids on Alumina." Science **245**: 845-847.
- Liua, Q.-Y., M. Coulombe, et al. (2000). "Synaptic connectivity in hippocampal neuronal networks cultured on micropatterned surfaces." Developmental Brain Research **120**: 223-231.
- Lucius, R., R. Mentlein, et al. (1998). "Riboflavin-Mediated Axonal Degeneration of Postnatal Retinal Ganglion Cells In Vitro is Related to the Formation of Free Radicals." Free Radical Biology & Medicine **24**: 798-808.
- Ma, W., J. J. Pancrazio, et al. (1998). "Neuronal and glial epitopes and transmitter-synthesizing enzymes appear in parallel with membrane excitability during neuroblastoma x glioma hybrid differentiation." Developmental Brain Research **106**: 155-163.
- May, K. M. L., Y. Wang, et al. (2004). "Development of a Whole-Cell-Based Biosensor for Detecting Histamine as a Model Toxin." Anal. Chem. **76**: 4156-4161.
- Mynlieff, M. (1999). "Identification of different putative neuronal subtypes in cultures of the superior region of the hippocampus using electrophysiological parameters." NEUROSCIENCE **93**: 479-486.
- Neher, E. and B. Sakmann (1992). "The patch clamp technique." Scientific American **266**: 44-51.
- Poeta, M., L. Riedel, et al. (2004). "Incorporation of 13F into DETA monolayer." In preparation.
- Powers, R. K. and M. D. Binder (2000). "Summation of Effective Synaptic Currents and Firing Rate Modulation in Cat Spinal Motoneurons." The Journal of Neurophysiology **83**: 483-500.
- Puleo, D. A. and A. Nanci (1999). "Understanding and controlling the bone-implant interface." Biomaterials **20**: 2311-2321.
- Ravenscroft, M.S., Bateman, K.E., et al., (1998). "Developmental Neurobiology Implications from Fabrication and Analysis of Hippocampal Neuronal Networks on Patterned Silane-Modified Surfaces," J. Amer. Chem. Soc. **120**:12169 (1998).
- Rekling, J. C., G. D. Funk, et al. (2000). "Synaptic Control of Motoneuronal Excitability." Physiological Reviews **80**: 767-852.
- Schaffner, A. E., J. L. Barker, et al. (1995). "Investigation of the factors necessary for growth of hippocampal neurons in a defined system." Journal of Neuroscience Methods **62**: 111-119.
- Schoenfisch, M. H., M. Ovadia, et al. (2000). "Covalent surface chemical modification of electrodes for cardiac pacing applications." Journal of Biomedical Materials Research **51**: 209 - 215.
- Stenger, D. A., J. J. Hickman, et al. (1998). "Microlithographic determination of axonal/dendritic polarity in cultured hippocampal neurons." Journal of Neuroscience Methods Volume **82**: 167-173.
- Tosatti, S., R. Michel, et al. (2002). "Self-Assembled Monolayers of Dodecyl and Hydroxy-dodecyl Phosphates on Both Smooth and Rough Titanium and Titanium Oxide Surfaces." Langmuir **18**: 3537 - 3548.
- Ulman, A. (1991). "Introduction to Ultrathin Organic Films ." Academic Press, Inc.: San Diego, CA.
- Weiss, P. S., H. Yokota, et al. (1998). "Creating, tailoring and using one-dimensional interfaces in two-dimensional films." J. Phys.: Condens. Matter **10**: 7703-7712.
- Wilcox, K. S., J. Buchhalter, et al. (1994). "Properties of inhibitory and excitatory synapses between hippocampal neurons in very low density cultures." Synapse **18**: 128-151.
- Williams, K. R. and R. S. Muller (1996). "Etch rates for micromachining processing." Microelectromechanical Systems, Journal of **5**: 256-269.
- Zhang, X., M. Yang, et al. (2004). "Detect-to-warn cell based sensing technology: Chemical sensing of multiple agents in a cascade." Materials Research Society Symposium Proceedings: 187-195.